

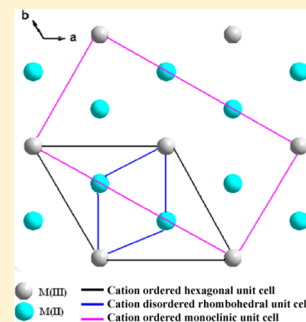
Layered Double Hydroxides: Proposal of a One-Layer Cation-Ordered Structure Model of Monoclinic Symmetry

K. Jayanthi, Supreeth Nagendran, and P. Vishnu Kamath*

Department of Chemistry, Central College, Bangalore University, Bangalore 560 001, India

Supporting Information

ABSTRACT: Layered double hydroxides are obtained by partial isomorphous substitution of divalent metal ions by trivalent metal ions in the structure of mineral brucite, $\text{Mg}(\text{OH})_2$. The widely reported three-layer polytype of rhombohedral symmetry, designated as polytype $3R_1$, is actually a one-layer polytype of monoclinic symmetry (space group $C2/m$, $a = 5.401 \text{ \AA}$, $b = 9.355 \text{ \AA}$, $c = 11.02 \text{ \AA}$, $\beta = 98.89^\circ$). This structure has a cation-ordered metal hydroxide layer defined by a supercell $a = \sqrt{3} \times a_0$; $b = 3 \times a_0$ ($a_0 =$ cell parameter of the cation-disordered rhombohedral cell). Successive layers are translated by $(1/3, 0, 1)$ relative to one another. When successive metal hydroxide layers are translated by $(2/3, 0, 1)$ relative to one another, the resultant crystal, also of monoclinic symmetry, generates a powder pattern corresponding to the polytype hitherto designated as $3R_2$. This structure model not only removes all the anomalies intrinsic to the widely accepted cation-disordered structure but also abides by Pauling's rule that forbids trivalent cations from occupying neighboring sites and suggests that it is unnecessary to invoke rhombohedral symmetry when the metal hydroxide layer is cation ordered. These results have profound implications for the correct description of polytypism in this family of layered compounds.



INTRODUCTION

Layered double hydroxides (LDHs) comprise positively charged metal hydroxide layers having the composition $[\text{M}^{\text{II}}_{1-x}\text{M}^{\text{III}}_x(\text{OH})_2]^{x+}$.¹ The operation of Pauling's rule,² which prohibits the M^{III} cations from occupying neighboring cation sites, limits the value of x to 0.33. At this composition, the M^{II} and M^{III} cations are ordered in the ab plane, giving rise to a supercell $a = \sqrt{3} \times a_0$, where a_0 is the lattice dimension of a cation-disordered metal hydroxide layer.

There is now considerable evidence both from spectroscopy as well as from diffraction studies of laboratory-synthesized (powder data)^{3–8} and mineral (single-crystal data)^{9,10} samples to support a cation-ordered structure model. Despite this, the overwhelming volume of diffraction studies^{11,12} have favored a cation-disordered structure model (space group $R\bar{3}m$, $a = 3.10 \text{ \AA}$, $c = 24\text{--}32 \text{ \AA}$). This widely accepted cation-disordered structure model has the following features.

- (1) The M^{II} and M^{III} cations are statistically distributed in a single crystallographically defined site.
- (2) The a parameter is close to that of mineral brucite, $\text{Mg}(\text{OH})_2$ ($a_0 = 3.13 \text{ \AA}$), from whose structure the LDH is derived by the partial isomorphous substitution of Mg^{2+} by M^{III} .
- (3) There is a single $(\text{M}^{\text{III}}, \text{M}^{\text{II}})\text{--O}$ distance conferring a D_{3d} coordination symmetry to the metal ion.
- (4) The array of hydroxyl ions has a hexagonal symmetry, whereby a single metal hydroxide layer can be described by the symbol "AbC" (A, B, C correspond to the positions of hydroxyl ions in a close packed array; b is the position of the metal ion).

- (5) The LDHs crystallize in a range of polytypes as described by Bookin and Drits.¹³ This range comprises crystals with one-, two-, and three-layer periodicities of hexagonal and rhombohedral symmetries designated by symbols $1H$, $2H_{1-3}$, $3R_{1-2}$, and $3H_{1-7}$.
- (6) The most widely prevalent polytypes among both laboratory and mineral samples are $1H$, $2H_1$, $3R_1$, and $3R_2$.^{13–15}

Over 100 structure refinements based on the cation-disordered structure model have been cited by Richardson in his elaborate reviews.^{11,12}

The cation-disordered structure model however has numerous infirmities of a very fundamental nature which cannot be ignored.

- (1) The ionic radii of trivalent cations are significantly smaller than those of divalent cations,¹⁶ whereby a credible structure model is not expected to be based on a single metal–oxygen bond length.
- (2) When $[\text{M}^{\text{II}}(\text{OH})_6]$ and $[\text{M}^{\text{III}}(\text{OH})_6]$ coordination polyhedra of different sizes share edges, the array of hydroxyl ions lose their hexagonal symmetry.¹⁷ There is a nonuniform distension of the hydroxyl ion network resulting in three in-plane nonbonded HO---OH interatomic distances.⁷
- (3) The packing of hydroxyl ions can no longer be described in terms of the close-packed positions A, B, C.

Received: May 14, 2015

Published: August 12, 2015

- (4) Given that a single metal hydroxide layer can no longer be described as an “AC” layer, an entirely new description of polytypism has to be developed.

Therefore, based on fundamental chemical considerations, it is imperative that a cation-disordered structure model is rejected. Two questions of vital importance arise.

- (1) How can the large mass of PXRD data^{11,12} that fit a cation-disordered structure model be reconciled with a cation-ordered structure? In particular, can the PXRD profiles hitherto attributed to a three-layer rhombohedral cell be generated by a cation-ordered crystal of lower symmetry?
- (2) Given a cation-ordered metal hydroxide layer,^{7,8} what are the different possible ways of stacking them one on top of another? In other words, how do we predict the complete universe of polytypes that could be generated by a cation-ordered layer?

In this manuscript we endeavor to find answers to these questions. We choose the LDHs of Zn²⁺ with Cr³⁺ and Al³⁺ as illustrative examples for the following reasons.

- (1) The LDHs of Zn²⁺ obtained by coprecipitation are better ordered than those of other divalent cations.
- (2) The [Zn–Cr–SO₄] LDH undergoes a 1H → 3R₁ transformation⁸ and is thereby an ideal LDH to investigate the relationship between the cation-ordered and the cation-disordered structure models.
- (3) The [Zn–Al–IO₃] LDH crystallizes in the structure of the rare 3R₂ polytype¹⁵ and provides a model for the other cation-disordered structure of rhombohedral symmetry predicted by Bookin and Drits.¹³

EXPERIMENTAL SECTION

The LDH samples studied here are more fully described elsewhere.^{8,15} Briefly, the [Zn–Cr–SO₄] LDH was precipitated under pH stat conditions (pH = 5) at 60 °C under flowing N₂. The [Zn–Al–IO₃] LDH was prepared by ion exchange starting from the [Zn–Al–NO₃] precursor. The anion exchange was carried out at 90 °C for 40 h. Chemical analysis yielded the formulas [Zn₂Cr(OH)₆][SO₄]_{10.5}·4H₂O and [Zn₂Al(OH)₆][IO₃]₂·2.1H₂O for the two samples. The LDHs were characterized by powder X-ray diffraction (PXRD) using a Bruker D8 Advance powder diffractometer (Cu Kα source, λ = 1.5418 Å). Data were collected over 5–90° 2θ (step size 0.02° 2θ; counting time 10 s per step). IR spectra and TGA data of the two samples are given in earlier papers.^{8,15}

The PXRD patterns were simulated using code DIFFaX. Within the DIFFaX formalism, a solid is treated as a stacking of layers of atoms, and the PXRD pattern is computed by integrating the diffraction intensity layer by layer. The position coordinates of the atoms within a single metal hydroxide layer were obtained from the cation-ordered structure model (space group *P*-3, *a* = 5.414 Å, *c* = 11.07 Å).⁸ Using this layer as the building block, the crystal was constructed using different stacking vectors. The crystal symmetry was declared as UNKNOWN. When this option is chosen, code DIFFaX evaluates the Laue symmetry. Stacking vectors that yielded crystals of monoclinic symmetry (Laue symmetry 2/*m*) were identified by means of these simulations. The very same stacking vectors were also found to generate PXRD profiles corresponding to the 3R₁ and 3R₂ polytypes.

For the purpose of Rietveld refinement, in the first instance, code FOX (Free objects for crystallography)¹⁸ was employed. A metal hydroxide layer obtained from a cation-ordered structure model of monoclinic symmetry was used as the partial structure, and the SO₄²⁻ ion was introduced into the interlayer space as a molecule. The position of the SO₄²⁻ ion was determined by refining the S-atom position in direct space. The goodness of fit parameters were used as the cost function in this Monte Carlo process. The structure model

obtained from FOX was input into code GSAS,¹⁹ and the refinement was continued by computing a series of difference Fourier maps to locate the oxygen atoms of the intercalated water molecules. Bond length constraints had to be imposed to obtain a stable refinement. Crystal structure visualization software was constantly used at all stages of the refinement to gauge the chemical reasonability of the structure.

RESULTS AND DISCUSSION

Of the three typical PXRD patterns (Figure 1) obtained from a cohort of LDH samples, the most widely reported pattern⁸

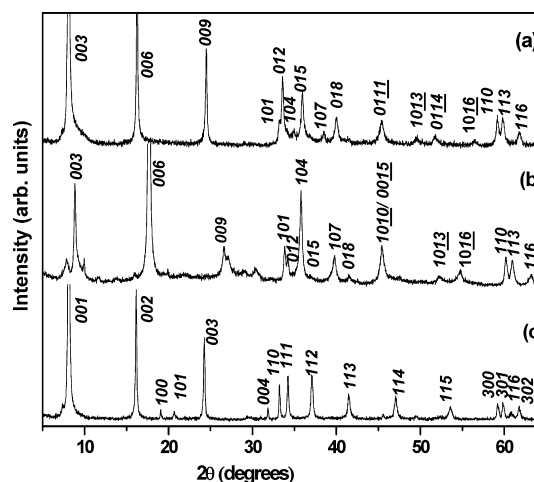


Figure 1. Observed PXRD patterns of the (a) 3R₁ polytype, (b) 3R₂ polytype, and (c) 1H polytype. (a and c) Different phases of the [Zn–Cr–SO₄] LDH, and (b) [Zn–Al–IO₃] LDH.

(trace a, in Figure 1) is indexed to a three-layer rhombohedral cell having an in-plane cell dimension *a*₀ ≈ 3.1 Å (Table S1). This value corresponds to a cation-disordered phase. The appearance of 01*l* (*l* = 2, 5, 8) reflections identifies this phase, within the Bookin and Drits scheme,¹³ as the 3R₁ polytype. Within this scheme, the stacking sequence of hydroxyl ions is AC=CB=BA=AC..., wherein A, B, and C stand for positions of hydroxyl ions in 2-D hexagonal nets rotated by *n* × 60° (*n* = 1, 3, 5) relative to one another, and “=” stands for a trigonal prismatic interlayer site (site symmetry *D*_{3h}).

The PXRD pattern in trace b (Figure 1) is also indexed to a three-layer rhombohedral cell of the same in-plane cell dimension (*a*₀ ≈ 3.1 Å), and the appearance of 10*l* (*l* = 1, 4, 7) reflections identifies the phase as the 3R₂ polytype. Within the Bookin and Drits scheme,¹³ the stacking sequence of hydroxyl ions is AC-BA-CB-AC..., wherein “-” stands for a trigonal antiprismatic interlayer site (site symmetry *D*_{3d}).

Given that these cation-disordered structures (*a*₀ ≈ 3.1 Å) are unrealistic, these assignments stand rejected. In contrast to these is trace c in Figure 1, which is indexed to a more realistic cell having an in-plane dimension *a* = 5.41 Å (√3 × *a*₀), suggestive of cation ordering in the *ab* plane. The appearance of 11*l* (*l* = 0, 1, 2, 3, 4, 5) reflections suggests a one-layer cell of hexagonal symmetry (polytype 1H).

The structure refined (space group *P*-3, *a* = *b* = 5.414 Å, *c* = 11.07 Å)⁸ by a Rietveld fit of the PXRD data at trace c in Figure 1 yields a metal hydroxide layer (Figure 2a) comprising [Zn(OH)₆] polyhedra in an ordered arrangement relative to the smaller [Cr(OH)₆] polyhedra. The metal hydroxide layer belongs to the layer group *p*-312/*m* (Figure 2b) and is adorned by a set of 3 and –3 axes. The 2-D array of hydroxyl ions does

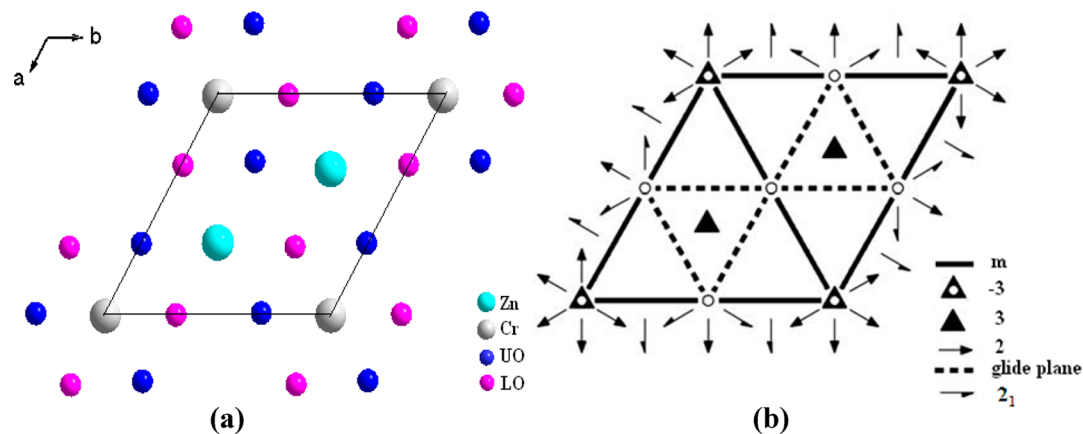


Figure 2. (a) Metal hydroxide layer of the $1H$ polytype viewed along the c axis, and (b) layer group representation of the corresponding structural synthon.

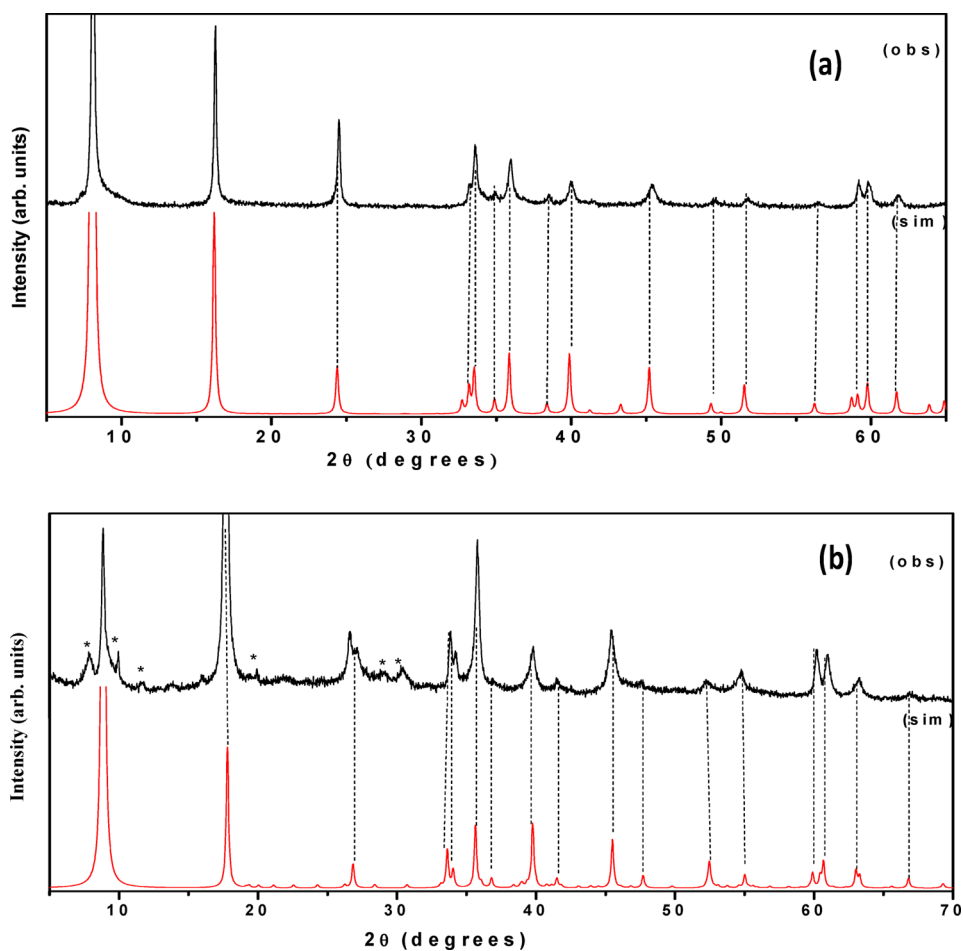


Figure 3. (a) Observed PXRD profile of the $3R_1$ polytype compared with the pattern simulated for the $1M_1$ polytype. (b) Observed PXRD profile of the $3R_2$ polytype compared with the pattern simulated for the $1M_2$ polytype. Features marked by the asterisk are due to impurities.

not have hexagonal symmetry any more, with three nonbonded in-plane HO---OH distances. The position of the hydroxyl ions cannot be described by the symbols A, B, and C, which is used to describe a close packing of atoms. Henceforth the stacking sequence of the metal hydroxide will be described in terms of the appearance of metal ions along the stacking direction.

The structure of the $1H$ polytype^{7,8} is obtained by stacking the metal hydroxide layers shown in Figure 2a one above another using the stacking vector $(0, 0, 1)$. In this structure the

Cr^{3+} (or Al^{3+}) ions lie along a straight line parallel to the stacking direction. The same is true of the Zn^{2+} ions. Other ways of stacking the metal hydroxide layers can be envisaged. The use of stacking vectors $(1/3, 2/3, 1)$ [or the symmetry equivalent $(2/3, 2/3, 1)$] and $(2/3, 1/3, 1)$ [or the symmetry equivalent $(1/3, 1/3, 1)$] lead to a structure where the stacking of metal ions is $-\text{Cr}\cdots\text{Zn}\cdots\text{Zn}\cdots\text{Cr}-$. All these stacking vectors result in structures in which the 3-fold axes of successive layers coincide to yield the $3R$ polytype (three layered unit cell of

rhombohedral symmetry). However, the computed PXRD patterns of the 3R polytypes (Figure S1) do not match with either of the patterns (traces a and b in Figure 1) ascribed to the cation-disordered structures. As there is no other way of stacking the metal hydroxide layer of Figure 2a in such a way as to conserve the 3-fold symmetry, we arrive at the inevitable conclusion that the phases corresponding to traces a and b in Figure 1 cannot possibly be of rhombohedral symmetry.

We then ask the question how do we stack the metal hydroxide layers in such a way as to obtain crystals of lower symmetry? In other words, how do we stack the metal hydroxide layer in such a way as to destroy the 3-fold out-of-plane symmetry while at the same time retaining the in-plane 2-fold axes. A possible way, adopting the structural synthon approach,²⁰ is to use the stacking vectors (1/3, 0, 1) or the symmetry related (0, 1/3, 1). Such a translation removes the coincidence of the 3-fold axes of successive layers. A DIFFaX simulation of the PXRD pattern leads to a profile that matches trace a in Figure 1 (Figure 3a). A related stacking vector (2/3, 0, 1) or the symmetry equivalent (0, 2/3, 1) generates a PXRD profile that matches with trace b in Figure 1 (Figure 3b). The Laue symmetry generated by the DIFFaX code for both simulations is 2/m, suggesting a monoclinic symmetry for the resultant crystals. Accordingly, the PXRD patterns at traces a and b in Figure 1 were indexed to single-layered cells of monoclinic symmetry (Table 1).

Table 1. Three-Layered Rhombohedral Polytypes Indexed to Single-Layered Polytypes of Monoclinic Symmetry

[Zn–Cr–SO ₄]		[Zn–Al–IO ₃]	
<i>a</i> = 5.42 Å		<i>a</i> = 5.32 Å	
<i>b</i> = 9.35 Å		<i>b</i> = 9.22 Å	
<i>c</i> = 11.02 Å		<i>c</i> = 10.15 Å	
β = 98.72°		β = 98.72°	
[Zn–Cr–SO ₄]		[Zn–Al–IO ₃]	
2 θ (obs)	<i>hkl</i>	2 θ (obs)	<i>hkl</i>
8.1	001	8.9	001
16.3	002	17.7	002
24.5	003	26.7	003
33.2	113	33.9	130
33.6	–131	35.9	004
34.9	131	39.9	033
36.0	–114	45.6	–142
38.5	–221	60.5	–314
40.0	–222	61.4	–330
45.5	–134		
49.5	232		
51.8	–241		
59.2	–136		
59.8	234		
61.8	251		

In conclusion, the PXRD patterns hitherto ascribed to cation-disordered 3R₁ and 3R₂ polytypes actually correspond to cation-ordered structures of monoclinic symmetry.

STRUCTURE REFINEMENT

A survey of the reported LDH structures yielded the following cation-ordered structure models of monoclinic symmetry.

- (1) The bayerite-based [LiAl₂(OH)₇]Cl·2H₂O LDH refined to a C2/m structure model (*a* = 5.097 Å, *b* = 8.82 Å, *c* = 7.69 Å, β = 101.103°) by Thiel and co-workers.²¹

- (2) The model proposed by Krivovichev and co-workers²² for mineral quintinite, a naturally occurring [Mg₄Al₂(OH)₁₂]CO₃·3H₂O LDH, also belonging to the space group C2/m (*a* = 5.266 Å, *b* = 9.114 Å, *c* = 7.766 Å, β = 103.17°).
- (3) Nickelalumite structure model (space group P2₁/n; *a* = 10.2567 Å, *b* = 8.8815 Å, *c* = 17.0989 Å, β = 95.548°) proposed for the Al-rich LDH of the formula [NiAl₄(OH)₁₂]SO₄·3H₂O.²³

Although the nickelalumite structure includes SO₄²⁻ ions in the interlayer as in the LDHs used in this work, we reject this model. The metal hydroxide layer in this LDH is an altogether different structural synthon (layer group *p*12₁/*a*1), containing as it does an ordered arrangement of cation vacancies. Our DIFFaX simulations show that the loss of rhombohedral symmetry is not due to any fundamental change within the metal–hydroxide layer but merely by a translation of successive layers relative to one another. Such a translation can be easily modeled by a suitable choice of β within a structure model of monoclinic symmetry. The metal hydroxide layers in the structure models belonging to the C2/m space group are very similar to that shown in Figure 2a. Therefore, a Le Bail fit of the PXRD profile given at trace a in Figure 1 was performed within the space group C2/m. In initial trials, *a* = 5.414 Å was chosen, the same as that in the cation-ordered hexagonal structure. The *b* = 9.365 Å was chosen to correspond to the Cr···Cr distance along the diagonal of the hexagonal cell, thereby establishing the topotactic relationship [110]_h||[010]_m (*h*, hexagonal; *m*, monoclinic) (Figure 4). The *c* parameter was fixed at the value

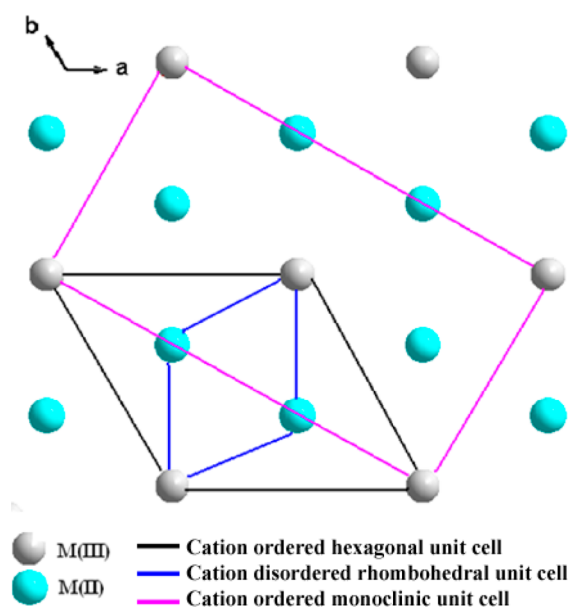


Figure 4. Topotactic relationship between the unit mesh of the hexagonal lattice (lines in black) and the corresponding monoclinic lattice (lines in magenta).

of the first basal reflection at 11.05 Å. The value of β was then varied over the range from 90° to 106° initially by increments of 0.5° and subsequently in increments of 0.25° in the range from 97° to 99°, until all observed Bragg reflections were generated. At each stage the background and profile parameters were refined, and finally, the cell parameters were refined to yield β = 98.72°.

To proceed further with structure refinement, at the initial stage, it is necessary to suitably model the metal hydroxide layer in partial construction of the structure model. Toward this end, the $[\text{LiAl}_2(\text{OH})_6]^+$ layer²⁰ was chosen and the $[\text{Zn}_2\text{Cr}(\text{OH})_6]^+$ layer was constructed by placing Cr^{3+} in the place of Li^+ and Zn^{2+} in the place of Al^{3+} . This layer had the oxygen atoms (O1 and O2) of the hydroxyl ions distributed in two sites, namely, the 8j and 4i. These O-atom positions were varied by hand using a crystal visualization software to obtain Zn–O and Cr–O distances comparable to those found in the cation-ordered 1H polytype.⁸ Once a satisfactory metal hydroxide layer was generated, it was introduced into code FOX as a partial structure model.

The SO_4^{2-} ion was introduced into the interlayer space as a molecule, wherein the S–O bond lengths and the O–S–O bond angles were held invariant. The SO_4^{2-} ion was allowed to diffuse in the interlayer region by a random variation in the position coordinates of the central S atom. In each position, the SO_4^{2-} ion was further rigidly rotated. A least-squares approach to minimize the error between the calculated and the observed pattern was adopted. To ensure speedy convergence and avoid physically unrealistic solutions, the diffusion of the SO_4^{2-} ions was restricted to a plane midway between the successive metal hydroxide layers. The oxygen atoms of sulfate O3–O6 were found to occupy 8j positions of a general nature. As FOX operates in the direct space, to locate the positions of the water molecules, the structure was exported to General Structure Analysis System (GSAS) to continue the refinement using the least-squares method.

The occupancy of the SO_4^{2-} ion was fixed according to chemical analysis to 0.125. Bond length (S–O = $1.45 \text{ \AA} \pm 0.1 \text{ \AA}$) and bond angle (O–S–O = $109.5^\circ \pm 8^\circ$) restraints were imposed on the SO_4^{2-} ion. The refinement was carried to completion. At this point, the difference profile still had certain residual features. A series of difference Fourier maps were evaluated to locate the positions of the intercalated water molecules. Difference Fourier maps indicated two different 8j positions (0.9675, 0.1572, 0.3942), (0.8764, 0.1725, 0.1875) and a 4i position (0.4467, 0.0000, 0.3940) as the likely site of intercalated water molecules. The difference Fourier map computed at this stage was devoid of any significant electron density. The Rietveld fit (Figure 5, Table 2) is satisfactory. The atom positions and the refined bond lengths and bond angles are given in Tables 3 and 4, respectively, and are also available from the Cambridge Crystallography Data Centre (CCDC 1063513).

Given the emerging consensus over cation ordering in the metal hydroxide layer, it is fruitful to compare the monoclinic structure model with the hexagonal polymorph which is identified as the 1H polytype.⁸ There are, in our opinion, three ways in which the hexagonal LDH crystal could distort to monoclinic symmetry.

- A major distortion of the $[\text{M}(\text{OH})_6]$ polyhedra by a Jahn–Teller kind of distortion, with the attendant consequences on the layer group symmetry of the metal hydroxide layer.
- Incorporation of anions of low molecular symmetry or by incorporation of anions in a low coordination symmetry in the interlayer.
- By an altered stacking of the metal hydroxide layers.

Although these factors are interrelated, each can be examined in turn to arrive at the major causative factor.

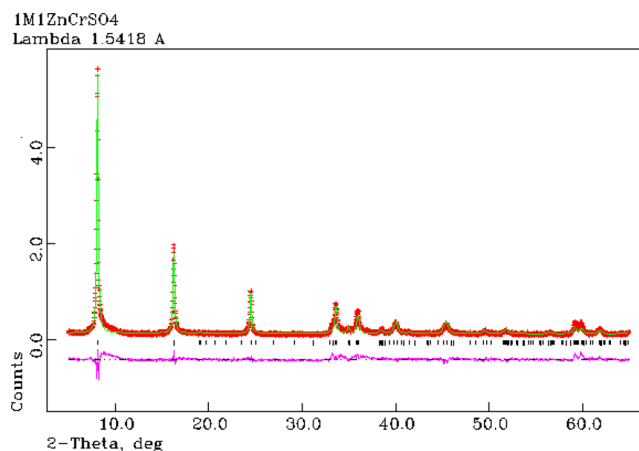


Figure 5. Rietveld fit of the PXRD pattern of the cation-ordered $[\text{Zn-Cr-SO}_4]$ LDH of monoclinic symmetry (broken line, red, observed data; continuous line, green, calculated data; magenta, difference profile). Vertical lines correspond to the positions of the Bragg reflections.

Table 2. Results of Rietveld Refinement of the Structure of the $[\text{Zn-Cr-SO}_4]$ LDH

molecular formula	$[\text{Zn}_4\text{Cr}_2(\text{OH})_{12}][\text{SO}_4] \cdot 8.4\text{H}_2\text{O}$
cryst syst	monoclinic
space group	$C2/m$
cell parameters (Å)	$a = 5.4013(18) \text{ \AA}; b = 9.3550(28) \text{ \AA}; c = 11.0185(12) \text{ \AA}$ $\alpha = \gamma = 90^\circ; \beta = 98.89^\circ$
vol. (Å ³)	552.26 Å
data points	3007
parameters refined	43
R_{wp}	0.1654
R_p	0.1396
$R(F^2)$	0.2032
reduced χ^2	4.612

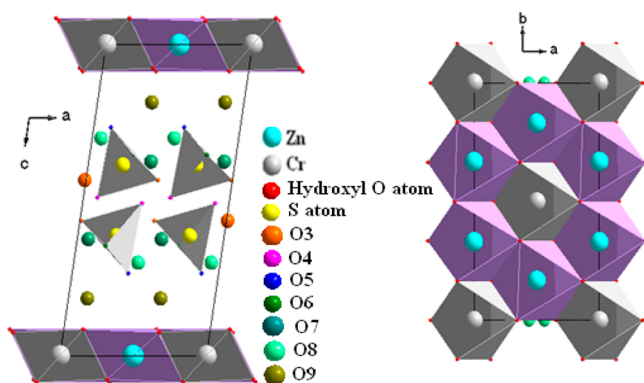
Table 3. Refined Atomic Position Parameters of $[\text{Zn-Cr-SO}_4]$ LDH

atom	Wyckoff position	x	y	z	SOF
Zn	4g	0	0.331(20)	0	1
Cr	2a	0	0	0	1
O1	8j	0.867(8)	0.1649(4)	0.085(13)	1
O2	4i	0.3448(15)	0	0.0756(32)	1
S	8j	0.2353(17)	0.906(7)	0.3861(9)	0.125
O3	8j	0.492(33)	0.97(22)	0.4346(17)	0.125
O4	8j	0.095(4)	0.9236(6)	0.4909(20)	0.125
O5	8j	0.117(6)	0.9594(34)	0.2653(24)	0.125
O6	8j	0.2854(6)	0.7528(25)	0.3535(33)	0.125
O7	8j	0.4516(9)	0.295(4)	0.3788(20)	0.780
O8	4i	0.5465(12)	0	0.3039(7)	0.550
O9	8j	0.371(14)	0.311(6)	0.1845(4)	0.020

The metal hydroxide layer in the monoclinic structure model proposed here (Figure 6) is not very different from that in the hexagonal structure, as the a and b parameters are directly obtained from the latter (Figure 4). The metal hydroxide layer in the hexagonal structure yields only one Cr(III)–O bond length (1.907 Å) and two Zn(II)–O bond lengths (2.041 and 2.063 Å). The coordination symmetries of Zn^{2+} and Cr^{3+} were evaluated using the code SYMGROUP²⁴ by including the six O

Table 4. Refined Bond Distances and Bond Angles of the $[\text{Zn-Cr-SO}_4]$ LDH

distances (Å)		angles (deg)	
Zn–O1	2.0194(4)	O1–Zn–O1	100.522(15)
Zn–O1	2.0571(7)	O2–Zn–O1	102.185(22)
Zn–O2	2.0131(4)	O2–Zn–O2	78.289(23)
Cr–O1	1.9959(4)	O1–Zn–O1	80.304(15)
Cr–O2	1.9190(7)	O1–Cr–O1	101.256(22)
O1–O2	2.4897	O1–Cr–O2	101.055(15)
O1–O1	2.6296	O3–S–O4	103.261(21)
O1–O1	2.5318	O4–S–O5	117.596(16)
S–O3	1.5288(5)	O5–S–O6	100.108(9)
S–O4	1.48540(34)	O6–S–O3	105.554(14)
S–O5	1.47157(30)	O3–S–O5	115.228(22)
S–O6	1.5121(4)		
Zn polyhedra			
O1–O2	3.2034		
O2–O1	3.1389		
O1–O2	3.1360		
Cr polyhedra			
O1–O2	3.0230		
O2–O1	3.0859		

**Figure 6.** Structure of the $1M_1$ polytype of the $[\text{Zn-Cr-SO}_4]$ LDH (a) viewed along the b axis showing the interlayer with a bilayer arrangement of sulfate ions and (b) viewed along the c axis showing two distinct sites for Cu and Cr atoms.

atoms coordinated to each of the two cations. Code SYMGROUP evaluates a score for each of the symmetry elements potentially extant in the coordination polyhedron. A score of zero shows the exactness with which the symmetry element exists. A high score indicates the absence of the corresponding symmetry element. While no strict quantitative limiting score is indicated, an examination of the score in any grouping yields a set of symmetry elements with a low score (0–0.08) and a set of symmetry elements with a high score (1–5). The former are readily seen to be present, while the latter are absent. This permits the evaluation of the approximate point group symmetry of the first coordination shell. The application of this procedure to the $1H$ structure of $[\text{Zn-Cr-SO}_4]$ LDH yields a coordination symmetry of the D_{3d} for $[\text{Cr}(\text{OH})_6]$ polyhedron and D_3 for $[\text{Zn}(\text{OH})_6]$ polyhedron (Table 5). For the $1M_1$ structure refined here, the $[\text{Cr}(\text{OH})_6]$ and $[\text{Zn}(\text{OH})_6]$ polyhedra yield D_{3d} and D_3/D_{3d} point group symmetries, respectively. These results clearly show that although the metal hydroxide layer in the $1M_1$ polytype yields two Cr(III)–O bond lengths and three Zn(II)–O bond lengths (Table 4) the distortion of the coordination polyhedra is only

slight; thereby, the lowering of crystal symmetry is not on account of the distortion in the metal coordination. The invariance of the metal hydroxide layer between the $1H$ and the $1M_1$ structures is also evident from the fact that the PXRD profile of the $1M_1$ was simulated using the layer extracted from the $1H$ structure (Figure 3). The origin of monoclinic symmetry is therefore clearly due to a change in the stacking vector.

The accretion of $[\text{M}(\text{OH})_6]$ coordination polyhedra of different sizes has a profound consequence on the array of hydroxyl ions in the crystal. In the cation-disordered rhombohedral structure model, the array of hydroxyl ions has a perfectly hexagonal symmetry with only one nonbonded, intralayer HO---OH contact distance, 3.12 Å. Such hexagonal arrays facilitate the description of OH positions in terms of close-packed positions, A, B, and C. In the $1H$ structure there are three in-plane HO---OH distances (Figure 7) with a deviation of 0.3 Å between the closest and farthest contacts. In the $1M_1$ polytype, this deviation is indeed lower at 0.18 Å, although several more contact distances are observed. In conclusion, the polytypes can no more be described in terms of the positions of the hydroxyl ions.

To explore the chief distinguishing feature between the proposed monoclinic polytypes, a SYMGROUP analysis of the symmetry of the interlayer site was carried out. This was done by including the hydroxyl ion positions lining the gallery and choosing six near neighbor hydroxyl ions, three from the upper and three from the lower array of hydroxyl ions. This yields a D_{3h} symmetry for the $1M_1$ polytype and D_{3d} for the $1M_2$ polytype (Table 5). Thus, in keeping with the views of Bookin and Drits,¹³ it is still possible to classify the newly identified polytypes by the local symmetry of their interlayer sites.

The only question that arises is why are there no additional reflections arising out of a lowering of the crystal symmetry? One possible reason could be the invariance of the metal hydroxide layer in the crystals of the two symmetries due to which no new hk reflections should be expected. Nevertheless, the powder pattern computed for the structure of the $1M_1$ polytype (Figure S2) reveals additional peaks of low relative intensity (0.1–0.9%) which are not observed. Some of the prominent peaks split into doublets which are included within the line width of the observed peaks.

From the foregoing discussion it is evident that authentic $3R_1$ and $3R_2$ polytypes are possible only within single-cation-layered phases such as the lithium cobalt oxides (LiCoO_2) and the birnessite type oxides of the type KMnO_2 .²⁵ In the former system these are referred to as P3 and O3 structures, respectively.²⁶

The evidence of cation ordering among the II–III LDHs calls for a comparison of the properties of this class of compounds with those of the $[\text{Li-Al}]$ LDHs, wherein cation ordering is firmly established. The $[\text{Li-Al}]$ LDHs are known to exhibit shape selectivity in the intercalation of anions.^{27–29} It is to be investigated if a similar capability is found in the II–III LDHs, in which case, the domain of their applications is considerably wider than currently presumed.

CONCLUSIONS

We show that the layered double hydroxides hitherto thought to crystallize with rhombohedral symmetry are actually crystals of monoclinic symmetry. The decrease in crystal symmetry occurs due to an alteration in the stacking vector. The altered

Table 5. Local Site Symmetries Computed by Code SYMGROUP for Different Sites in the 1H and 1M₁ Structures

symmetry of the [M(OH) ₆] polyhedra			
1M ₁ polytype [Zn(OH) ₆]		1H polytype [Zn(OH) ₆]	
symmetry elements	scores	symmetry elements	scores
C ₃	0.0647	C ₃	0.0000
3C ₂	0.0000, 0.0485, 0.04858	3C ₂	0.0031, 0.0031, 0.0031
mirror planes (3σ _d)	0.0573, 0.05732, 0.0910	mirror planes (3σ _d)	0.2065, 0.2065, 0.2065
S ₆	0.10095	S ₆	0.2096
i	0.09100	i	0.2096
D _{3d} /D ₃ point group		D ₃ point group	
[Cr(OH) ₆]		[Cr(OH) ₆]	
symmetry elements	scores	symmetry elements	scores
C ₃	0.0332	C ₃	0.0000
3C ₂	0.0000, 0.0249, 0.0249	3C ₂	0.0000, 0.0000, 0.0000
mirror planes (3σ _d)	0.0000, 0.0249, 0.0249	mirror planes (3σ _d)	0.0000, 0.0000, 0.0000
S ₆	0.0332	S ₆	0.0000
i	0.0000	i	0.0000
D _{3d} point group		D _{3d} point group	
local symmetry of the interlayer site			
1M ₁ polytype		1M ₂ polytype	
symmetry elements	scores	symmetry elements	scores
C ₃	0.08688	C ₃	0.01597
3C ₂	0.03560, 0.03794, 0.07134	3C ₂	0.0000, 0.01198, 0.01198
mirror planes (1σ _h and 3σ _v)	0.01207, 0.03397, 0.04296,	mirror planes (3σ _d)	0.00716, 0.00716,
	0.07528		0.01538
S ₃	0.08041	S ₆	0.01789
i	3.46943	i	0.01538
D _{3h} point group		D _{3d} point group	

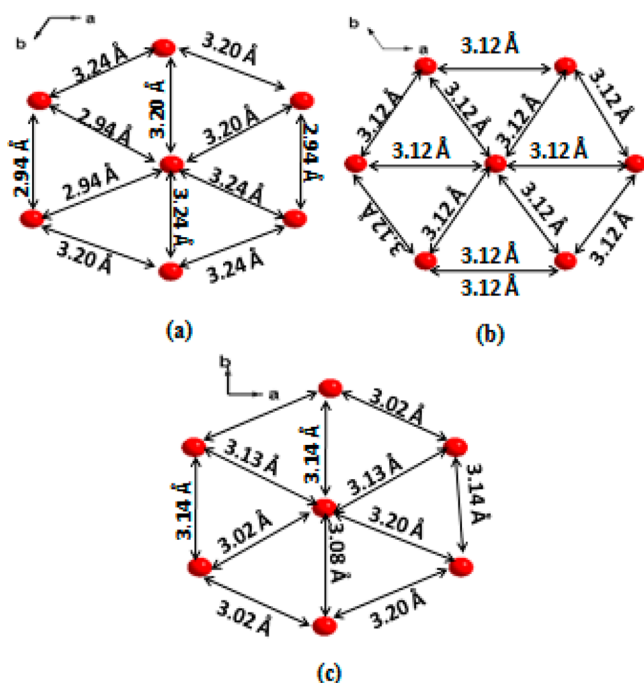


Figure 7. Array of hydroxyl ions in (a) cation-ordered 1H-polytype, (b) cation-disordered 3R₁-polytype, and (c) cation-ordered 1M₁-polytype.

stacking sequence destroys the 3-fold symmetry normal to the metal hydroxide layer.

■ ASSOCIATED CONTENT

Supporting Information

The Supporting Information is available free of charge on the ACS Publications website at DOI: 10.1021/acs.inorgchem.5b01050.

Observed 2θ values of 3R₁, 3R₂, and 1H polytypes with their corresponding indices obtained from PROZKI; DIFFaX-simulated patterns of the [Zn–Cr–SO₄] LDH using different stacking vectors; observed PXRD pattern of [Zn–Cr–SO₄] compared with the POWDERCELL simulation using the structure data of the 1M₁ polytype (PDF)

■ AUTHOR INFORMATION

Corresponding Author

*E-mail: vishnukamath8@hotmail.com.

Notes

The authors declare no competing financial interest.

■ ACKNOWLEDGMENTS

We thank Dr. S. Radha for providing the LDH samples for this study and the Department of Science and Technology (DST), Government of India (GOI), for financial support. K.J. is a Project Fellow supported by a University Grants Commission (UGC) of India funded Major Research Project. S.N. is a recipient of a Junior Research Fellowship (NET) of the UGC. P.V.K. is a recipient of the Ramanna Fellowship of the DST.

■ REFERENCES

- Reichle, W. T. *Solid State Ionics* **1986**, *22*, 135–141.

- (2) Pauling, L. *J. Am. Chem. Soc.* **1929**, *51*, 1010–1026.
- (3) Roussel, H.; Briois, V.; Elkaim, E.; de Roy, A.; Besse, J. P. *J. Phys. Chem. B* **2000**, *104*, 5915–5923.
- (4) Bigey, L.; Depege, C.; de Roy, A.; Besse, J. P. *J. Phys. IV* **1997**, *7* (C2), 949–950.
- (5) Sideris, P. J.; Nielsen, U. G.; Gan, Z.; Grey, C. P. *Science* **2008**, *321*, 113–116.
- (6) Sideris, P. J.; Blanc, F.; Gan, Z.; Grey, C. P. *Chem. Mater.* **2012**, *24*, 2449–2461.
- (7) Jayanthi, K.; Kamath, P. V. *Dalton Trans.* **2013**, *42*, 13220–133230.
- (8) Radha, S.; Kamath, P. V. *Inorg. Chem.* **2013**, *52*, 4834–4841.
- (9) Cooper, M. A.; Hawthorne, F. C. *Can. Mineral.* **1996**, *34*, 91–97.
- (10) Humincki, D. M. C.; Hawthorne, F. C. *Can. Mineral.* **2003**, *41*, 79–82.
- (11) Richardson, I. G. *Acta Crystallogr., Sect. B: Struct. Sci., Cryst. Eng. Mater.* **2013**, *B69*, 150–162.
- (12) Richardson, I. G. *Acta Crystallogr., Sect. B: Struct. Sci., Cryst. Eng. Mater.* **2013**, *B69*, 414–417.
- (13) Bookin, A. S.; Drits, V. A. *Clays Clay Miner.* **1993**, *41*, 551–557.
- (14) Allmann, R. *Acta Crystallogr., Sect. B: Struct. Crystallogr. Cryst. Chem.* **1968**, *B24*, 972–979.
- (15) Radha, S.; Prasanna, S. V.; Kamath, P. V. *Cryst. Growth Des.* **2011**, *11*, 2287–2293.
- (16) Shannnon, R. D. *Acta Crystallogr., Sect. A: Cryst. Phys., Diffraction, Theor. Gen. Crystallogr.* **1976**, *A32*, 751–767.
- (17) Radha, S.; Jayanthi, K.; Breu, J.; Kamath, P. V. *Clays Clay Miner.* **2014**, *62*, 53–61.
- (18) Fox, *Free Objects for Crystallography*; <http://objcryst.sourceforge.net>.
- (19) Larson, A. C.; Von Dreele, R. B. *Los Alamos National Laboratory Report LAUR* **2004**, 86–748.
- (20) Britto, S.; Kamath, P. V. *Inorg. Chem.* **2011**, *50*, 5619–5627.
- (21) Thiel, J. P.; Chiang, C. K.; Poeppelmeier, K. R. *Chem. Mater.* **1993**, *5*, 297–304.
- (22) Krivovichev, S. V.; Yakovenchuk, V. N.; Zhotova, E. S.; Zolotarev, A. A.; Pakhomovsky, Y. A.; Ivanyuk, G. Yu. *Mineral. Mag.* **2010**, *74*, 833–840.
- (23) Uvarova, Y. A.; Sokolova, E.; Hawthorne, F. C. *Can. Mineral.* **2005**, *43*, 1151–1519.
- (24) Casanova, D.; Alemany, P.; Alvarez, S. *SYMOP*; Universidad de Barcelona: Barcelona, Spain, 2007.
- (25) Drits, D. A.; Lanson, B.; Gaillot, A.-C. *Am. Mineral.* **2007**, *92*, 771–88.
- (26) Delmas, C.; Braconnier, J.-J.; Hagenmuller, P. *Mater. Res. Bull.* **1982**, *17*, 117–23.
- (27) Fogg, A. M.; Green, V. M.; Harvey, H. G.; O'Hare, D. *Adv. Mater.* **1999**, *11*, 1466–1469.
- (28) Fogg, A. M.; Dunn, J. S.; Shyu, S.-G.; Cary, D. R.; O'Hare, D. *Chem. Mater.* **1998**, *10*, 351–355.
- (29) Lei, L.; Millange, F.; Walton, R. I.; O'Hare, D. *J. Mater. Chem.* **2000**, *10*, 1881–1886.